NEW ALGORITHMS FOR MICROWAVE MEASUREMENTS OF OCEAN WINDS

Frank J. Wentz
Remote Sensing Systems
475 Gate Five Rd., Sausalito, California 94965, USA

Steve Peteherych
Atmospheric Environment Service
4905 Dufferin Street, Downsview, Ontario M3H5T4, Canada

ABSTRACT

Improved second generation wind algorithms are used to process the three month SEASAT SMMR and SASS data sets. The new algorithms are derived without using in situ anemometer measurements. All known biases in the sensors' measurements are removed, and the algorithms' model functions are internally self-consistent. The computed SMMR and SASS winds are collocated and compared on a 150 km cell-by-cell basis, giving a total of 115444 wind comparisons. The comparisons are done using three different sets of SMMR channels. When the 6.6H SMMR channel is used for wind retrieval, the SMMR and SASS winds agree to within 1.3 m/s over the SASS primary swath. At nadir where the radar cross section is less sensitive to wind, the agreement degrades to 1.9 m/s. The agreement is very good for winds from 0 to 15 m/s. Above 15 m/s, the off-nadir SASS winds are consistently lower than the SMMR winds, while at nadir the high SASS winds are greater than SMMR's. When 10.7H is used for the SMMR wind channel, the SMMR/SASS wind comparisons are not quite as good. When the frequency of the wind channel is increased to 18 GHz, the SMMR/SASS agreement substantially degrades to about 5 m/s.

1. INTRODUCTION

Aircraft and satellite experiments have clearly demonstrated that the wind speed near the sea surface can be remotely sensed by microwave radiometers and scatterometers [Swift, 1977; Munn, 1978; Bernstein, 1982]. The passive radiometer collects the radiation that is naturally emitted by the sea surface and intervening atmosphere, whereas the active scatterometer measures the component of transmitted power that is backscattered from the sea surface. Both the emitted and backscattered radiation are directly affected by surface roughness, which is correlated with the near-surface wind speed. The correlation of roughness and wind speed is a complex, coupled phenomenon [Kinsman, 1965]. Ocean roughness is first generated by atmospheric pressure fluctuations and tangential wind shears. The newly generated waves then transfer energy to other ocean wavelengths, which in turn affect the wind flow.

The oceanographic satellite SEASAT carried a multi-frequency microwave radiometer SMMR and a 14.6 GHz scatterometer SASS [Weissman, 1980]. The wind speeds inferred by these two sensors agreed with in situ anemometer measurements to within about 2 m/s [Jones et al., 1982; Wentz et al., 1982]. Better agreement (1.4 m/s) was obtained when the SMMR winds were directly compared to the SASS winds. This good agreement for the SMMR/SASS comparisons indicated a high correlation exists between the types of roughness sensed by the two instruments.

These original SMMR/SASS wind comparisons were limited to a series of case studies over the Northeast Pacific and the North Atlantic during two weeks in

September 1978. The wind retrieval algorithms were carefully tuned for this time period and region, and the resulting wind comparisons looked very promising. However, when extending the comparisons to all oceans for the entire three month life of SEASAT, these first generation algorithms proved to be biased and overly complex. For example, the SMMR algorithm was plagued with temporal brightness temperature (T_B) drifts and with relative T_B biases that varied across the swath [Bernstein and Morris, 1983]. Also the algorithm attempted to use all the SMMR channels, even though not enough was known about the relative error statistics of the various channels. The SASS algorithm produced winds that had an artificial cross swath variation [Wentz et al., 1984]. Furthermore, the winds retrieved from the horizontal polarization radar cross section (σ^0) measurements did not agree with those coming from the vertical polarization σ^0. Finally, σ^0's corresponding to low winds were systematically filtered out, and as a result the winds below 6 m/s were biased high.

In this investigation, we use improved second generation wind algorithms to process the three month SMMR/SASS data set. A unique feature of these algorithms is that their derivations do not require in situ anemometer measurements. Thus the algorithm winds are a true satellite product, not affected by problematic conventional observations. In addition, the SMMR and SASS algorithms are developed independently of each other. All known biases in the T_B's and σ^0's are removed, and the algorithms' model functions are internally self-consistent. The resulting retrieval techniques are more accurate and simpler than their forerunners.

The computed SMMR and SASS winds are collocated and compared on a cell-by-cell basis. The cell resolution is 150 km, which corresponds to the SMMR footprint size for the lowest resolution 6.6 GHz channel. A total of 115444 wind comparisons are made over SEASAT's three months. These comparisons are stratified according to four swath positions going from nadir to the outer portion of the swath. To determine the wind sensing performance of various radiometer configurations, the comparisons are done using three different combinations of SMMR channels.

2. SMMR GEOPHYSICAL ALGORITHM

The retrieval of wind speed and other geophysical parameters from SMMR T_B measurements is accomplished by solving a set of simultaneous equations:

$$T_{Bi} = f_i(T_s, W, V, L) \qquad (1)$$

where T_{Bi} is the SMMR measurement for the i th channel and $f_i(\cdots)$ is the corresponding model function. The unknown variables are sea-surface temperature T_s (K), wind speed W (m/s), atmospheric water vapor V (g/cm^2), and atmospheric liquid water L (g/cm^2). The SMMR T_B model function was first derived by Wentz [1983a], and later the wind-induced emissivity term ΔE was modified [Wentz, 1984]. In the original model, ΔE came from 119 collocated SMMR T_B cells and SASS wind speeds for two SEASAT passes over the North Pacific. Because of the small size of this data set and problems with the earlier versions of the SASS winds, ΔE was rederived. The new derivation is based on 32213 SMMR T_B cells and is independent of SASS winds. In addition, no in situ anemometer measurements are required in the new derivation. The new ΔE's are approximately the same as those obtained for the earlier model.

The original SEASAT SMMR geophysical algorithm [Wentz et al., 1982] used all ten SMMR channels. With ten observations and four unknowns, the system of equations (1) is over-determined, and a least-squares technique was used to find T_s, W,

V, and L. Although the least-squares algorithm performed better than regression algorithms [Lipes and Born, 1981], there was a drawback. A weight must be assigned to each channel. This weight represents the inverse of the expected variance between the observation and the model function. In general, the lower frequency channels should be weighted more heavily than the higher frequencies. Unfortunately, not enough is currently known about the error statistics of the observations or model function to determine the correct weights. In view of this, we decided to simplify the inversion problem and deal with a deterministic set of equations.

A deterministic algorithm for finding T_s, W, V, and L consists of solving a set of four simultaneous model function equations. As explained below, a good choice for the four channels is 6.6V, 6.6H, 18V, and 21V (6.6V denotes 6.6 GHz, vertical polarization). The model function is quasi-linear in terms of T_s, W, V, and L, and a unique solution exists for the system of four equations. This solution is found by Newton's iterative method extended to four dimensions. Only two or three iterations are required for convergence. The performance of the four parameter algorithm was first tested by comparing the retreived T_s with Reynolds' [1982] SST climatology. The rms difference was 1.58 C when the SST's for 31781 individual SMMR cells were compared to the climatology [Wentz, 1983b].

In this paper we are only interested the wind speed retrieval, not SST. To estimate the wind speed, we use a three channel algorithm (6.6H/18V/21V), rather than the four channel algorithm discussed above. The variable T_s is set equal to Reynolds' SST climatology, which is given on a one month by 1^0 latitude by 1^0 longitude grid. The climatology SST is interpolated to the center of the SMMR cell. Once T_s is specified, there are only three unknowns, and hence only three channels are required by the inversion algorithm. We select the three channel algorithm because it is simpler, requires fewer radiometer channels, and is as accurate as the four channel algorithm in determining W. Typically, the difference between the climatology SST and the true SST is about 1.5 C, which causes only a 0.6 m/s error in the retrieved wind. To verify this, we compare wind speeds coming from the 6.6H/18V/21V algorithm with those coming from the 6.6V/6.6H/18V/21V algorithm. The rms difference is 0.7 m/s. Furthermore, when compared to the SASS winds, the three channel algorithm shows slightly better agreement than the four channel algorithm (rms of 1.3 m/s compared to 1.4 m/s).

To minimize the retrieval error, the algorithm's three channels are selected such that a given channel has a high sensitivity to one variable and low sensitivity to the other two variables. In this way, the determinant for the system of equations is maximized. Horizontal polarization is used to infer wind speed because it is more sensitive to surface roughness than vertical polarization. Conversely, vertical polarization is used to determine V and L. The best frequency for wind speed determination is 6.6 GHz, which is least affected by atmospheric interference. Thus 6.6H is selected for the wind speed channel. The 18V channel is chosen for liquid water determination. This channel is better than the 37V channel because it does not saturate as fast with increasing L. Furthermore, 37 GHz is more susceptible to errors caused by variations in the rain drop size distribution and by rain cells that do not fill the SMMR footprint. Finally, the obvious selection for the water vapor channel is 21V, which is on the water vapor absorption line.

In addition to the 6.6H/18V/21V algorithm, we also analyze the performance of a 10.7H/18V/21V algorithm and a 18H/18V/21V algorithm. The purpose of changing the wind speed channel from 6.6H to 10.7H and 18H is to compare the performance of

different radiometer systems. For example, the microwave radiometer SSM/I to be launched in 1985 aboard the DMSP Block 5D-2 satellite operates at four frequencies: 19, 22, 37, and 85 GHz. Thus the performance of the 18H/18V/21V algorithm will provide some information on the SSM/I wind sensing capability.

3. SASS WIND ALGORITHM

The retrieval of wind speed from SASS σ^0 measurements is performed in a way analogous to that described in Section 2 for the SMMR. We solve a set of two simultaneous equations that equate the σ^0 measurement to the SASS model function. Wentz et al. [1984] derived the following function for the ocean radar cross section at the SASS frequency of 14.6 GHz:

$$\sigma^0 = A_0 + A_1 \cos(X-X_w) + A_2 \cos[2(X-X_w)] \qquad (2)$$

The angles X_w and X are azimuth angles for the wind direction and σ^0 measurement, respectively. The A coefficients are known functions of the incidence angle and wind speed W. The derivation of A_0 and A_2 is based on the statistics of the SASS observations, and no in situ anemometer measurements are required. The A_1 coefficient comes from aircraft circle measurements of σ^0. The statistically derived model is free of the incidence angle and polarization relative biases that occurred in the earlier version of the model function [Schroeder et al., 1982], which was tuned to the JASIN anemometer measurements.

In computing the SASS winds, we only use vertical polarization observations, which constitute 88% of all observations. Excluding horizontal polarization simplifies the retrieval problem and subsequent analysis. A collocation algorithm finds all SASS measurements that fall within a given SMMR 150 km cell. The SMMR swath is on the starboard side of the satellite subtrack. Except at nadir, the SASS measurements will come from either the forward starboard antenna (beam 1) or the aft starboard antenna (beam 2). The azimuth angles X for all measurements in a 150 km cell coming from the same beam are essentially the same, and the following averages are computed:

$$\langle\sigma^0\rangle_i = \langle A_0\rangle_i + \langle A_1\rangle_i \cos(X_i-X_w) + \langle A_2\rangle_i \cos[2(X_i-X_w)] \qquad (3)$$

where $\langle\cdots\rangle_i$ represents an average over the measurements coming from beam i, i = 1 or 2, and X_i is the azimuth angle for beam i. For nadir observations, the SASS measurements come from all four antennas. Since A_1 and A_2 equal zero for the nadir σ^0, these measurements are averaged together irrespective of beam number.

The preaveraging of σ^0 before retrieving wind speed increases the signal-to-noise ratio (SNR). In a 150 km cell in the middle of the SASS primary swath, there are typically 9 observations from each beam. Averaging these observations increases the SNR by a factor of 3. For light winds below 6 m/s, the SNR is poor, and the preaveraging helps considerably. In the original SASS algorithm [Jones et al., 1982], no preaveraging was done. The low SNR measurements were simply excluded from processing, which resulted in data gaps in low wind speed areas and a positive bias in the retrieved wind speeds for moderate wind speed areas.

Equation (3) represents two equations in two unknowns, W and X_w. The equations are solved by noting that the azimuth angles for the forward and aft antennas are nearly orthogonal ($X_2 = X_1 + 90° \pm 1°$). Using this orthogonality property, the second harmonic in the two equations is eliminated, giving

$$\langle A_2\rangle_2 \langle\sigma^0\rangle_1 + \langle A_2\rangle_1 \langle\sigma^0\rangle_2 = \langle A_2\rangle_2 \langle A_0\rangle_1 + \langle A_2\rangle_1 \langle A_0\rangle_2 + \varepsilon \quad (4)$$

$$\varepsilon = \langle A_2\rangle_2 \langle A_1\rangle_1 \cos(X_1 - X_w) - \langle A_2\rangle_1 \langle A_1\rangle_2 \sin(X_1 - X_w) \quad (5)$$

The term ε arises because there is a difference between an upwind and downwind measurement of σ^0. If the upwind and downwind σ^0 were equal, then A_1 would be zero. For vertical polarization, which is used herein, the upwind-downwind difference is quite small, and ε can be treated as an error. Setting the term to zero gives

$$F(W) = \langle A_2\rangle_2 \langle\sigma^0\rangle_1 + \langle A_2\rangle_1 \langle\sigma^0\rangle_2 - \langle A_2\rangle_2 \langle A_0\rangle_1 - \langle A_2\rangle_1 \langle A_0\rangle_2 = 0 \quad (6)$$

The only unknown in the function F(W) is wind speed W, which is found by Newton's iterative method. Only two or three interations are required for convergence. The wind speed error introduced by neglecting ε is approximately

$$\Delta W = -\varepsilon / [\partial F(W)/\partial W] \quad (7)$$

For vertical polarization, $\Delta W/W$ is typically about 2%.

Once W is found, it can be substituted back into (3), and X_w can be calculated. The harmonic properties of (3) produce multiple solutions for X_w, which are called aliases. The number of these solutions is between 0 (no solution) and 4. This procedure gives a good estimate of the alias wind directions. However, to be exact, each alias has a slightly different wind speed solution because of the upwind-downwind term ε, and the wind speed coming from (6) cannot be applied to the individual aliases. Although the term ε is different for each alias, its average over the various aliases is nearly zero. Thus the average wind speed error ΔW is also zero, and the wind speed coming from (6) equals the average of the alias wind speeds. As such, it is the best estimate of wind speed that can be obtained if there is no additional dealiasing information, which is the case for this investigation. Fortunately, we are only interested in obtaining the wind speed and do not have to deal with the alias problem or the exact solution for X_w.

4. RESULTS

In this section, the collocated SMMR and SASS winds are compared. The SMMR and SASS swaths overlap on the starboard side of the satellite subtrack. The overlap area extends 600 km out from the subtrack and is divided into four 150 km square resolution cells. Beginning with the subtrack cell, these cells are numbered 1 through 4. The SMMR T_B measurements uniformly cover each cell, but the SASS σ^0 measurements do not. For cell 1, we only use the nadir SASS measurements that are restricted to a 40 km wide strip along the subtrack. The near-nadir SASS measurements at incidence angles of 4° and 8° are not used because they are relatively insensitive to wind speed. Cell 2 is also only partially filled with SASS observations. There is a gap in the SASS swath for incidence angles between 10° and 20°, and as a result the left half of cell 2 does not contain any SASS observations. The outer cells 3 and 4 are completely within the SASS primary swath and are uniformly filled with SASS measurements.

The SMMR antenna does a conical scan such that the incidence angle is a constant 49°. Thus the same physics and model function applies to cells 1 through 4. The only difference is that significant polarization coupling occurs in the edge cells 1 and 4. This polarization coupling makes the decoupled T_B values noisier for the edge cells. In contrast, the SASS antennas are fixed sticks, and each cell

corresponds to a different range of incidence angles. The SASS measurements in cell 1 are nadir observations for which σ^0 decreases with wind speed W approximately as $(1/W)^{\frac{1}{2}}$. For cell 2 the average incidence angle is about 25°, and σ^0 increases linearly with wind speed. For the two outer cells, σ^0 increases as the square of wind speed. Thus the SASS model function is quite different for the four cells. In view of this, the SMMR/SASS wind comparisons are stratified according to cell number. We expect that the best comparisons will occur for cell 3. For this cell, there is uniform coverage of both SMMR and SASS observations, the signal-to-noise ratio for SASS is the best, σ^0 is most sensitive to wind speed, and the polarization coupling for SMMR is a minimum.

For the 6.6H/18V/21V system, wind comparisons are done for the entire three month SEASAT mission. However, only nighttime observations are used because sea-surface sun glitter and Faraday rotation degrade the daytime SMMR data. Furthermore, the SMMR observations must be at least 800 km from land to avoid antenna sidelobe contamination. As a final filtering criteria, when the liquid water content L coming from the SMMR algorithm exceeds 50 mg/cm², which corresponds to a 0.5 mm/hr rain, the observation is excluded. The same filtering criteria are used for the 10.7H/18V/21V and 18H/18V/21V systems, except that only data coming from the second half of the SEASAT mission are used because of a problem with the 18 GHz channels. In the middle of the mission, the 18H and 18V channels experienced a sudden 4 K to 5 K drop in the mean T_B level. This drop is probably due to an unexpected change in the transmissivity of a SMMR waveguide component. Since the two higher frequency systems are rather sensitive to errors in the 18 GHz channels, we choose to avoid the problem and only use observations occurring in the second half of the mission after the 18 GHz anomaly. The wind retrieval from the 6.6H/18V/21V system is less sensitive to errors in the 18V T_B, and we correct the problem, as much as possible, by adding a time step bias to the 18V T_B so that the entire mission can be processed. A small linear time-dependent bias is also added to the 6.6H T_B to compensate for an observed 1.5 K drift over the three months.

Table 1 shows the summary statistics for the wind comparisons for the three radiometer systems. For cells 1 through 4, the table gives the number of observations, the mean SASS wind, the mean SMMR wind, and the standard deviation of the SMMR wind minus the SASS wind. As expected the 6.6H/18V/21V system gives the best results. The agreement between the SMMR and SASS winds for cells 2 through 4 is between 1.3 and 1.4 m/s and degrades to 1.9 m/s for nadir cell 1. Averaged over the three months, the mean wind speed should be nearly the same for the four cells. This is the case except that the SASS cell 2 winds appear to be about 0.5 m/s high relative to the other three cells. Also the SMMR cell 1 winds seem to be running about 0.3 m/s too high. These small cross swath wind variations are probably due to residual biases in the observations and in the SASS model function. The results for the 10.7H/18V/21V system are about the same as for the 6.6H/18V/21V system except that the SMMR/SASS wind agreement is somewhat poorer, being about 1.7 m/s for the off-nadir cells and 2.5 m/s for cell 1. Also, the mean SMMR wind is about 0.8 m/s lower than that for the 6.6H/18V/21V system. A substantial degradation in performance occurs for the 18H/18V/21V system. The wind agreement for cells 2 through 4 worsen to about 5 m/s, and cell 1 shows a 7.1 m/s variation between SMMR and SASS. The large discrepancy for cell 1 may be due to the fact that this cell is particularly affected by polarization coupling.

Table 1. SMMR/SASS Wind Comparisons

6.6H/18V/21V System	Cell 1	Cell 2	Cell 3	Cell 4
Number of Observations	31320	28714	28043	27367
Mean SASS Wind (m/s)	7.5	7.9	7.4	7.3
Mean SMMR Wind (m/s)	7.8	7.5	7.4	7.4
Std. Dev. SMMR-SASS (m/s)	1.9	1.4	1.3	1.4

10.7H/18V/21V System	Cell 1	Cell 2	Cell 3	Cell 4
Number of Observations	15031	13605	13164	12643
Mean SASS Wind (m/s)	7.1	7.7	7.2	7.0
Mean SMMR Wind (m/s)	7.1	6.7	6.6	6.4
Std. Dev. SMMR-SASS (m/s)	2.5	1.7	1.7	1.8

18H/18V/21V System	Cell 1	Cell 2	Cell 3	Cell 4
Number of Observations	14904	13592	13158	12613
Mean SASS Wind (m/s)	7.1	7.7	7.2	7.0
Mean SMMR Wind (m/s)	7.8	7.2	7.3	7.8
Std. Dev. SMMR-SASS (m/s)	7.1	4.5	4.7	5.2

Figure 1 shows the SMMR/SASS wind comparisons for the three radiometer systems and the four cells. In generating these plots, the observations are stratified into 1 m/s SASS wind speed bins. For each bin the mean SASS wind, the mean SMMR wind, and the standard deviation of SMMR winds are computed. The error bars in the plots are centered on these mean wind values. The length of the error bars equals the $\pm$ one standard deviation of SMMR winds. An error bar for moderate winds represents thousands of observations. For the extreme low and high winds, the number of observations for an error bar drops to between 5 and 100. For the 6.6H/18V/21V system, the agreement for low to moderate winds is quite good. However for winds above 15 m/s, the SASS winds are lower than the SMMR winds for the off-nadir cells and are higher than the SMMR winds for the nadir cell. There is no additional information to determine which is more correct, SMMR or SASS. However, in passing we note that the discrepancy at high winds cannot be corrected by simply adjusting the SMMR model function because the model and the physics are the same for cells 1 through 4. On the other hand, the SASS model function could be adjusted to remove the high wind discrepancy. At nadir, the sensitivity of σ^0 to high wind speeds could be increased, and off nadir the sensitivity could be decreased. Such an adjustment would be a departure from the constant power law model that is commonly used.

The 10.7H/18V/21V system shows the same trends as the 6.6H/18V/21V system except that the error bars are a little larger. However, going to the 18H/18V/21V system we see very large error bars. The apparent problem with the high frequency system is the difficulty in separating atmospheric effects from wind effects. The 18H wind channel is quite sensitive to atmospheric liquid water and water vapor.

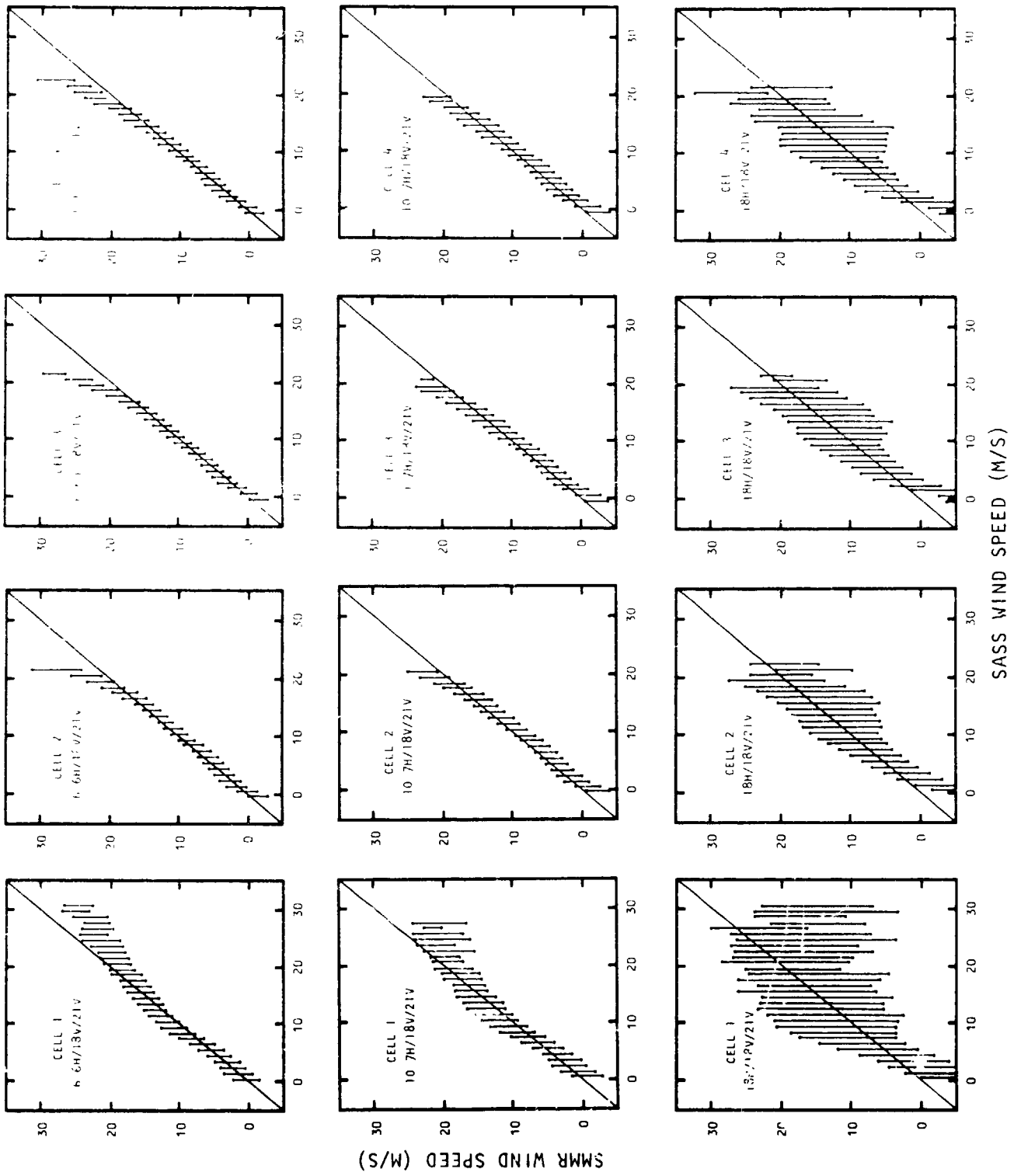

Fig. 1. A comparison of SMMR and SASS winds for three radiometer systems. Each row of plots corresponds to a particular radiometer system. The four plots in a row correspond to the cell swath position. Cell 1 is along the satellite subtrack and Cell 4 is at the outer portion of the swath.

5. SUMMARY AND CONCLUSIONS

Improved second generation algorithms are used to compute wind speeds for the SMMR and SASS over the three month life of SEASAT. When 6.6H is used for the SMMR wind channel, the winds coming from the two sensors agree to within 1.3 m/s over the SASS primary swath. At nadir where the radar cross section is less sensitive to wind, the agreement degrades to 1.9 m/s. The agreement is very good for low and moderate winds (0 to 15 m/s), and it thus appears that the SMMR can accurately measure winds even when there is no whitecapping. For winds above 15 m/s, the off-nadir SASS winds are consistently lower than the SMMR winds, while at nadir the high SASS winds are greater than the SMMR winds.

The SMMR/SASS wind agreement degrades a little when 10.7H is used as the wind speed channel, rather than 6.6H. When the frequency of the wind channel is increased to 18 GHz, the agreement is much worse, being 5 m/s over the SASS primary swath. This poor agreement is due to the difficulty in separating wind effects from atmospheric effects at 18 GHz. This separability problem is due to the fact that wind speed and atmospheric liquid water have nearly the same polarization signature at 18 GHz. Recent results show that if 37 GHz is used, rather than 18 GHz, the wind sensing performance is substantially improved. For example, the winds coming from a 37H/37V/21V configuration show about a 2.5 m/s agreement when compared to the SASS winds. The microwave radiometer SSM/I to be launched in 1985 aboard the DMSP Block 5D-2 satellite will operate at 19, 22, 37, and 85 GHz. Our results indicate that a 37H/37V/21V SSM/I wind algorithm will perform much better than a 19H/19V/21V algorithm.

We emphasize that the good agreement obtained in the 6.6H SMMR versus SASS comparisons does not necessarily mean that the actual wind speed can be measured to a 1.3 m/s accuracy. Rather, the results indicate that there exists a high correlation between the sea-surface roughness characteristics that affect microwave brightness temperatures and radar cross sections. Unfortunately, these inter-sensor comparisons do not really address the complex boundary layer problem involving the correlation of near-surface winds and sea-surface roughness.

Based on the results of this study, a number of recommendations are made:

(1) We recommend that users of the SEASAT SMMR and SASS geophysical products obtain the new second generation data sets, which are a substantial improvement over the first generation products released in 1981.

(2) The new SEASAT winds should be compared with all available in situ anemometer measurements so that the correlation between wind speed and surface roughness can be better quantified. Previous comparisons of SEASAT winds with in situ were clouded by the fact that the wind algorithms, which had many degrees of freedom, were initially tuned to the in situ.

(3) Potential users need to understand the capabilities and limitations of SSM/I. More study is required to determine the wind sensing performance of this important new sensor.

(4) Two-scale scattering theory should be compared to the SMMR and SASS model functions. In derivation of the models, wind speed sensitivities as functions of frequency, polarization, and incidence angle are obtained from the statistics of the SMMR and SASS observations, rather than theory. The question to be answered is whether or not the two-scale theory is consistent with the model functions.

6. ACKNOWLEDGMENTS

This research was supported by NASA's Oceanic Processes Program under Contract NASW-3606. Additional support for investigating the SSM/I performance was provided by NORDA's Remote Sensing Branch under Contract N00014-83-C-0520. We are also grateful to the Canadian Atmospheric Environment Service for generously providing computer support. We thank L. McGoldrick of NASA Headquarters and J. Hawkins of NORDA for making this investigation possible.

7. REFERENCES

Bernstein, R.L. (ed), 1982: Seasat Spec. Issue I, J. Geophys. Res., 87, 3173-3438.

Bernstein, R.L. and J.H. Morris, 1983: Tropical and mid-latitude North Pacific sea surface temperature variability from the SEASAT SMMR. J. Geophys. Res., 88, 1877-1891.

Jones, W.L., L.C. Schroeder, D.H. Boggs, E.M Bracalente, R.A. Brown, G.J. Dome, W.J. Pierson, and F.J. Wentz, 1982: The SEASAT-A satellite scatterometer: the geophysical evaluation of remotely sensed wind vectors over the ocean. J. Geophys. Res., 87, 3297-3317.

Kinsman, B., 1965: Wind Waves, 543-583, Prentice-Hall, New Jersey.

Lipes, R.G. and G.H. Born (ed), 1981: SMMR Mini-Workshop IV, JPL Tech. Rept. 622-234, Jet Propulsion Laboratory, Pasadena, California.

Munn, R.E. (ed), 1978: Boundary-Layer Meteorology, 13, 1-429.

Reynolds, R.W., 1982: A monthly averaged climatology of sea surface temperature. NOAA Tech. Rep. NWS 31, National Weather Service, Silver Spring, Maryland.

Schroeder, L.C., D.H. Boggs, G. Dome, I.M. Halberstam, W.L. Jones, W.J. Pierson, and F.J. Wentz, 1982: The relationship between wind vector and normalized radar cross section used to derive SEASAT-A satellite scatterometer winds. J. Geophys. Res., 87, 3318-3336.

Swift, C.T. (ed), 1977: IEEE J. of Oceanic Engineering, OE-2, 1-159.

Weissman, D.E. (ed), 1980: IEEE J. of Oceanic Engineering, OE-5, 71-182.

Wentz, F.J., V.J. Cardone, and L.S. Fedor, 1982: Intercomparison of wind speeds inferred by the SASS, Altimeter, and SMMR. J. Geophys. Res., 87, 3378-3384.

Wentz, F.J., 1983a: A model function for ocean microwave brightness temperatures. J. Geophys. Res., 88, 1892-1908.

Wentz, F.J., 1983b: Comparison of sea surface temperature retrievals using 6.6 and 10.7 GHz, RSS Tech. Rept., Remote Sensing Systems, Sausalito, California.

Wentz, F.J., 1984: Modifications to brightness temperature model function, RSS Tech. Rept., Remote Sensing Systems, Sausalito, California.

Wentz, F.J., S. Peteherych, and L.A. Thomas, 1984: A model function for ocean radar cross sections at 14.6 GHz. To be published in J. Geophys. Res.